Search for a Permanent Electric Dipole Moment on the ^{129}Xe Atom

T. G. Vold, F. J. Raab, B. Heckel, and E. N. Fortson
Department of Physics, University of Washington, Seattle, Washington 98195
(Received 30 March 1984)

A measurement of a permanent electric dipole moment on xenon atoms has yielded the null result $d(^{129}\mathrm{Xe}) = (-0.3 \pm 1.1) \times 10^{-26}\ e \cdot \mathrm{cm}$, achieved by use of spin exchange with optically pumped rubidium atoms to determine the precession frequency of the xenon nuclear spins as a function of applied electric field. This measurement improves the limit on an atomic dipole moment by over four orders of magnitude. It is sensitive to time-reversal–asymmetric forces within the atom, setting a new upper limit of $10^{-6}G_F$ on a short-range tensor-pseudotensor electron-nucleon coupling.

PACS numbers: 32.80.Bx, 11.30.Er, 35.10.Di

The discovery[1] in 1964 of *CP* nonconservation in the K_0 meson system provided the first and still the only evidence of time-reversal (T) symmetry violation. In attempting to find other examples of T nonconservation accurate searches have been undertaken for a permanent electric-dipole moment (edm) on an elementary particle or atomic system. Measurements on the neutron[2,3] have yielded the important null value for the dipole moment, $d(n) < 4 \times 10^{-25}\ e \cdot \mathrm{cm}$. Searches for an edm on atoms and molecules have set upper limits on T-nonconserving electron-nucleon forces, and on the edm of the electron and the proton.[4-8].

We report here the first result in a new search[9] for an atomic edm. We observe precession of the nuclear spins of xenon atoms in a magnetic field, and measure the change in precession frequency when an applied electric field is reversed relative to the magnetic field. Thus far we have obtained the null result:

$$d(^{129}\mathrm{Xe}) = (-0.3 \pm 1.1) \times 10^{-26}\ e \cdot \mathrm{cm}, \tag{1}$$

where the quoted error is statistical and one standard deviation. This result is sensitive to several plausible T-nonconserving forces within the atom. For example, it improves the limit on a tensor-pseudotensor interaction[5,8] between electrons and nucleons by over a factor of 10.

The ground state of ^{129}Xe is doubly degenerate, with the states distinguished by the axial nuclear-spin quantum number, $m_I = \pm\frac{1}{2}$. In external electric and magnetic fields E and B, the energy operator is $H = -\vec{\mathrm{d}} \cdot \vec{\mathrm{E}} - \vec{\mu} \cdot \vec{\mathrm{B}}$, where $\vec{\mathrm{d}} = d\vec{\sigma}$, $\vec{\mu} = \mu\vec{\sigma}$ are the electric and magnetic dipole operators. H gives a difference $\Delta\Omega = 4dE/\hbar$ in precession frequencies between $\vec{\mathrm{E}}$ parallel and antiparallel to $\vec{\mathrm{B}}$. If the precession is measured for the duration of its $1/e$ coherence lifetime τ with a signal to noise ratio S/N, and the procedure is repeated for a total time T, then a dipole can be measured with an accuracy of

$$\delta d = h[4E(2\tau T)^{1/2}(S/N)]^{-1}. \tag{2}$$

In this work, $\tau \cong 500$ sec, $S/N \cong 5000$, and $E \cong 4.5$ kV/cm, requiring $T \cong 20\,000$ sec to reach the observed uncertainty $\delta d \cong 10^{-26}\ e \cdot \mathrm{cm}$.

A schematic diagram of the experimental apparatus is given in Fig. 1. The xenon nuclei are polarized and their precession analyzed by spin exchange with optically pumped rubidium vapor.[10,11] A relatively large pump field, $B_{\mathrm{pump}} = 10$ mG, is applied parallel to the light for about 500 sec. A semiconductor laser with a 3-mW output tuned to the D_1 line of Rb (795 nm) polarizes the Rb at a rate of 50 sec^{-1}, while the depolarization rate, due mainly to collisions with Xe, is about 500 sec^{-1}, resulting in a Rb polarization of about 10%. A comparable Xe polarization builds up through a spin-exchange interaction with Rb that is enhanced[11] by formation of Rb-Xe van der Waals molecules.

After the Xe polarization is established, B_{pump} is turned off and a weak precession field, $B_{\mathrm{prec}} \cong 0.1$ mG, is applied perpendicular to the light. At this value, the Larmor frequency of the Rb is approximately equal to its depolarization rate so that its polarization retains a large projection parallel to the light. By contrast, the Xe spins precess freely at their Larmor frequency $\Omega/2\pi \cong 0.1$ Hz producing a net rotating magnetization that slowly decays away. The polarization and decay times for the Xe, $\tau \cong 500$ sec, are primarily determined by spin exchange with the Rb. The relaxation time due to all other sources is about 2000 sec, probably dominated by magnetic field inhomogeneities.

The Xe Larmor frequency is measured by observing the rotating Xe magnetization, with use of the polarized Rb as part of a magnetometer.[10] The sensitivity to the Xe magnetization comes from spin-spin interaction in Rb-Xe collisions. An oscillating magnetic field, B_{osc} is applied perpendicular to both

© 1984 The American Physical Society

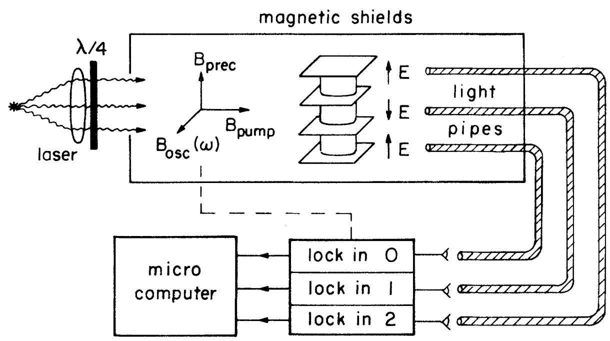

FIG. 1. A schematic view of the experimental apparatus.

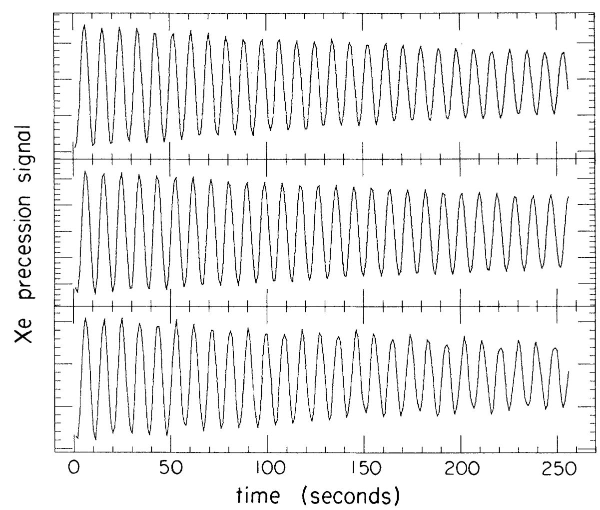

FIG. 2. The xenon magnetization along $B_{\rm osc}$ as a function of time for the top, center, and bottom cells, respectively, showing the precession and transverse relaxation of the ^{129}Xe nuclear spins. Solid straight lines connect the raw data points, which are digitized output voltages (in arbitrary units) from the lock-in amplifiers.

the light and $B_{\rm prec}$, with a frequency $\omega/2\pi = 300$ Hz, causing the Rb polarization in the plane perpendicular to $B_{\rm osc}$ to oscillate by approximately ± 1 rad about its equilibrium position along the light axis. In this way, the transmitted light becomes sensitive to any small Rb spin precession about the $B_{\rm osc}$ axis. The magnetometer signal is the modulation of the transmitted light at ω. If there is no static magnetic field parallel to $B_{\rm osc}$, the transmitted light amplitude is modulated only at 2ω, while a small static field or Xe magnetization parallel to $B_{\rm osc}$ will cause the average direction of the Rb polarization to be rotated slightly from the direction of the light, producing modulation at ω.

The cells are made of 11-mm lengths of 25-mm-diam Pyrex tubing with the electrodes (platinum-coated flat Pyrex end plates) glued in place with Torr-Seal epoxy. The interiors are coated with a siliconizing material, SurfaSil (formerly called Drifilm), to reduce relaxation of the Xe due to wall collisions and to prevent an electrically conducting monolayer of Rb from forming on the cylinder walls. They are filled with 2 Torr of natural xenon (26% ^{129}Xe), 220 Torr of nitrogen, and approximately 1 mm^3 of natural rubidium. The nitrogen is added to increase the electric breakdown potential.

Three such cells are stacked coaxially along $B_{\rm prec}$. Electric fields are applied along $B_{\rm prec}$ in one direction in the center cell and in the opposite direction in the two outer cells. Measurements of the optical Stark shift of the Rb atoms inside the cells corroborate the value of electric field calculated from the applied voltage. A regulated heater maintains the cells at the temperature (about 65 °C) required for the desired Rb vapor density (about 10^{-5} Torr), a compromise between a higher density with improved S/N and a lower density with a longer xenon coherence time τ. The cells, heater, and coils for applying $B_{\rm pump}$ and $B_{\rm prec}$ are located inside three concentric cylindrical Molypermalloy magnetic shields.

A pair of lenses and a plastic quarter-wave retarder transform the diverging, linearly polarized laser output into a 4-cm $\times$ 1.5-cm circularly polarized collimated beam that passes through holes in the magnetic shields and irradiates the cells. The light transmitted through each cell is channeled with plastic light fibers to p-i-n photodiode detectors outside of the shields.

The signals from the three photodiodes are analyzed with lock-in amplifiers referenced to ω. The lock-in outputs, proportional to the amplitude of the Xe polarization along $B_{\rm osc}$, are digitized and recorded by a computer at regular intervals, typically 1 sec. Figure 2 shows this Xe precession signal from each of the three cells, recorded simultaneously over a 256-sec interval. The frequency of the Xe precession, Ω, and coherence time τ are evident in the raw data. Most of the actual edm data were taken with somewhat improved signals having a longer lifetime $\tau \cong 500$ sec.

This digitized record constitutes one data set. Frequencies are determined by fitting with a separate exponentially decaying sine function for each cell. The process of pumping and measuring is repeated, alternating the sign of E and changing other parameters from one data set to the next. The fractional frequency difference between the center cell and the average of the outer cells,

$\Delta = (\Omega_c - \overline{\Omega}_0)/(\Omega_c + \overline{\Omega}_0)$, is calculated for each data set. Δ depends linearly on d, but is independent of variations in $B_{\rm prec}$ and its first space derivatives. We do in fact observe variations in Δ because the higher-order space derivatives of $B_{\rm prec}$ vary in relative magnitude from one data set to the next. The difference in $B_{\rm prec}$ between adjacent cells is typically 1 μG and exhibits fluctuations of about 10 nG from one data set to the next which are largely nonrandom. For instance, we observe long-term drifts and steps in the field distribution which are correlated with temperature changes and mechanical vibrations of the magnetic shields.

The known sources of noise as given by Eq. (2) include laser noise at the frequency of $B_{\rm osc}$ (300 Hz), causing white noise at the lock-in output, and magnetic field fluctuations at the Xe precession frequency (0.1 Hz), causing amplitude fluctuations in the Rb magnetometer. As mentioned above, there are additional nonrandom variations in Δ on a time scale comparable to the electric field flips. Because these variations are not correlated with the sign of E, we find that averaging alternating electric field sequences $(+ - - +)$ to obtain d reduces the scatter in d by as much as an order of magnitude. The observed scatter in d is then comparable to the prediction of Eq. (2), where S/N is determined by the fitting routine. The results of all our edm measurements, stretching over a ten week period, are shown in Table I.

TABLE I. Results of all edm measurements on ^{129}Xe.

Run[a]	$\tau_{\rm obs}$[b] (sec)	C_λ[c]	E (kV/cm)	$d(^{129}\mathrm{Xe})$[d] ($10^{-26}\ e\cdot$cm)
1	512	$\pm$	4.4	0.0 ± 5.6
2	512	$\pm$	4.4	0.0 ± 5.8
3	512	$\pm$	4.4	6.3 ± 4.9
4	512	$\pm$	4.4	-18.9 ± 12.6
5	256	$-$	3.2	1.0 ± 17.6
6	256	$-$	3.4	-13.2 ± 10.8
7	512	$-$	3.4	4.1 ± 3.5
8	512	$+$	3.4	3.7 ± 3.4
9	512	$+$	4.3	-1.0 ± 3.4
10	512	$-$	4.3	-1.7 ± 2.7
11	512	$-$	4.9	-3.4 ± 2.0
12	512	$+$	4.9	4.5 ± 4.0
	Weighted average			-0.3 ± 1.1

[a]Each run contains between 30 and 75 individual data sets taken on a single day. The twelve runs were taken over a ten week period.

[b]The observation time per data set, during which the ^{129}Xe precession signal is recorded and the precession frequency determined. In runs 5 through 12, the sign of E was reversed midway through $\tau_{\rm obs}$.

[c]Circular polarization of the light.

[d]Quoted errors are one standard deviation, determined by the scatter in the data.

Potential systematic errors could be caused by magnetic fields from asymmetric current leakage between the electrodes, and by any change with E reversal of quantities such as the component of the Rb magnetization along $B_{\rm prec}$. Auxiliary measurements show that these spurious effects should not contribute at the present level of accuracy.

Major improvements are being implemented which should increase S/N and reduce the susceptibility to systematic effects. An important advance will be to compare two atoms with spin-$\frac{1}{2}$ nuclei, such as ^{129}Xe and ^{199}Hg. Spin-$\frac{1}{2}$ systems are not sensitive to spurious electric quadrupole effects. Placing the atoms in the same cell allows magnetic perturbations of the precession frequencies to be divided out. It may become possible to approach the purely shot-noise–limited S/N, which would increase the present sensitivity by over four orders of magnitude.

Turning to an interpretation of our results, we first consider a P- and T-nonconserving short-range interaction between electrons and quarks, which would perturb the electronic wave functions and generate an edm. A T-nonconserving pseudo-tensor-tensor contact interaction,[5,8] can be written as

$$H_T = (C_T i G_{\rm F}/\sqrt{2}) \sum_{n,e} (\bar{\psi}_n \gamma_5 \sigma_{\mu\nu} \psi_n)(\bar{\psi}_e \sigma^{\mu\nu} \psi_e), \tag{3}$$

where $\psi_{n,e}$ are the nucleon, electron wave functions, γ_5 and $\sigma^{\mu\nu}$ are Dirac matrixes, $G_{\rm F}$ is the Fermi weak interaction coupling constant, and C_T is a parameter measuring the strength of this interaction. Using Eq. (3), a calculation[12] with a relativistic Hartree-Fock model of xenon including core shielding converts the measured edm in Eq. (1) to the upper limit $C_T < 10^{-6}$. A Thomas-Fermi treatment, also including shielding, agrees with this limit to within 30%.[13]

Our measurement is also sensitive to an intrinsic edm of the electron or of the nucleus. In general, the sensitivity grows rapidly with atomic number Z.[5,13] Because xenon has a $^1S_0$ configuration, an edm on individual electrons will give an atomic edm to ^{129}Xe only through a second-order effect, with the magnetic-dipole hyperfine interaction and the interaction of d_e with the nuclear Coulomb field as the perturbations.[14] A pseudoscalar-scalar interaction[5,7] similar to Eq. (3) enters in second order also. An edm of the nucleus, due either to nucleon-nucleon (quark-quark) P and T nonconservation,[15] or to an individual nucleon edm, can induce an edm in the atom as a whole because of incomplete shielding by the atomic electrons of an external electric field at the site of a nucleon.[5]

Analysis and evaluation of each of these effects in xenon is presently underway, and will appear in a forthcoming publication.[13]

We gratefully acknowledge the help of Robert Morley, Frank Hellinger, and Steve Lamoreaux in various stages of the experiment. This work is supported by National Science Foundation Grant No. PHY8203512A01.

[1] J. H. Christenson, J. Cronin, V. L. Fitch, and R. Turlay, Phys. Rev. Lett. **13**, 138 (1964).

[2] N. F. Ramsey, Rep. Prog. Phys. **45**, 95 (1982).

[3] I. S. Alterev *et al.*, Phys. Lett. **102B**, 13 (1981).

[4] P. G. H. Sandars, Phys. Lett. **14**, 194 (1965).

[5] P. G. H. Sandars, in *Atomic Physics, Vol. 4,* edited by G. zu Putlitz, E. W. Weber, and A. Winnacker (Plenum, New York, 1975), p. 71; L. I. Schiff, Phys. Rev. **132**, 2194 (1963).

[6] I. B. Khriplovich, Zh. Eksp. Teor. Fiz. **71**, 51 (1976) [Sov. Phys. JETP **44**, 25 (1976)].

[7] C. Bouchiat, Phys. Lett. **57B**, 184 (1975).

[8] E. A. Hinds and P. G. H. Sandars, Phys. Rev. A **21**, 471,480 (1980); D. E. Wilkening, N. F. Ramsey, and D. J. Larsen, Phys. Rev. A **29**, 425 (1984).

[9] T. G. Vold, F. J. Raab, and E. N. Fortson, Bull. Am. Phys. Soc. **27**, 37 (1982) (Abstracts No. HE2 and No. HE3).

[10] C. H. Volk *et al.*, Phys. Rev. A **21**, 1549 (1980); B. Grover, Phys. Rev. Lett. **40**, 391 (1978).

[11] N. D. Bhaskar, W. Happer, M. Larsson, and X. Zeng, Phys. Rev. Lett. **50**, 105 (1983); W. Happer, E. Miron, S. Schaefer, D. Schreiber, W. A. van Wijngaarden, and X. Zeng, to be published; see also, C. C. Bouchiat, M. A. Bouchiat, and L. C. Pottier, Phys. Rev. **181**, 3144 (1969).

[12] Ann-Marie Märtensson-Pendrill, private communication.

[13] T. G. Vold and E. N. Fortson, to be published.

[14] E. N. Fortson, Bull. Am. Phys. Soc. **28**, 1321 (1983).

[15] G. Feinberg, Trans. N.Y. Acad. Sci. **38**, 6 (1977); W. C. Haxton and E. M. Henley, Phys. Rev. Lett. **51**, 1937 (1983).